

Preparation of C30 Concrete Using Lead-Zinc Tailings

Xiaoying Liang^a, Dongxia Yuan^{a*}, Changlong Wang^{a,b,c}, Shenhua Jiao^d, Yuyan Zhang^e

^aSchool of Civil Engineering, Hebei University of Engineering, Handan 056038, China

^bJiangxi Key Laboratory of Mining Engineering, Jiangxi University of Science and Technology, Ganzhou 341000, China

^cTianjin Sunenergy Sega Environmental Science & Technology Co. Ltd, Tianjin 300000, China

^dChina Ordnance Industry Survey and Geotechnical Institute, Beijing 100053, China

^eChina Center for Information Industry Development of MIIT Institute of Industry Energy Conservation and Environment Protection, Beijing 100846, China
81057244@qq.com

This paper examines the feasibility of preparing C30 concrete with replacing part of cementitious materials with lead-zinc tailings (LZT). The optimal fineness of LZT is determined based on fineness measurement of the ground powder and the strength tests of mortars. C30 concrete is mixed partially replacing cement, fly ash (FA) and ground blast furnace slag (GBFS) with the LZT with the optimal fineness, respectively. The related properties of the concrete are measured. The concrete with LZT partially replacing cement, FA or GBFS can meet the requirements of C30 pump concrete. The concrete with LZT shows good durability. Based on the results of permeability, carbonation resistance and autogenous shrinkage tests, it indicates that the ground LZT show good micro-filler effect and pozzolanic reactivity in concrete since more than 60 % particles of LZT is smaller than 5 μm .

1. Introduction

The amount of industrial solid wastes has been vast for a long period in China, while the majority is mining tailings. According to the incomplete statistics, the overall amount of all kinds of tailings is 16 billion tons, one third of which belongs to iron ore tailings. The numerous stack of tailings brings the society the issues about natural resources, ecological environment, residential safety and land occupations (Wang et al., 2016). Although the secondary utilization of tailings has been worldly emphasized, the utilization rate is lower than 10% in China (Bobylev, 2009). Tailings are difficult to be used in the traditional building materials due to its nature finesses. It has been reported that tailings can be used to prepare building materials such as high-strength concrete (Ugama et al., 2014; Shetty et al., 2014), cementitious materials or cement, autoclaved lime-sand brick (Liu et al., 2016), glass-ceramics (Wang et al., 2015), autoclaved aerated concrete (Cui et al., 2017; Zhang et al., 2016) and so on. As a new type of high technology concrete, high performance concrete (HPC) represents the future of concrete technology, its durability has obtained a dramatic improvement compared to traditional concrete, which shows that concrete has marched towards high technology materials (Nematollahi and Sanjayan, 2014; Zhao et al., 2015). Mineral admixtures have become the sixth essential component for high technology concrete, in which fly ash (FA) is the most widely used mineral admixtures. FA can reduce bleeding of fresh concrete, lower the hydration heat, and improve the durability and long-term strength of concrete (Upadhyaya et al., 2015; Anastasiou et al., 2014). C30 concrete is most used concrete in civil construction in China, and it is usually ready-mixed and pumped to the construction sites in practice. However, the amount of cementitious materials is required to be more than 350 kg m^{-3} , or it would bring difficulty in pumping and problems on bleeding, segregation and other degradations. The further improvements in workability, mechanical properties and durability requires the amount of cementitious materials to be higher than 400 kg m^{-3} . This would increase the cost if only Portland cement is used, while it would also bring negative influence on the development of green and low- CO_2 emission concrete. With considering the shortage of FA and granulated blast furnace slag in some individual areas, it is important to develop low-cost green cementitious materials with ore tailings for the local infrastructure construction.

There are few reports about preparing HPC using lead-zinc tailings (LTZ) to partially replace cementitious materials. This paper examines the micro-filler effect and pozzolanic reactivity of ground LTZ since the LTZ after secondary mineral processing is already with fine particles which is easy for grinding. In this paper LTZ partially replaces cement, FA and GBFS in commercial concrete and its properties are evaluated.

2. Materials and Experimental methods

2.1 Materials

Lead-zinc tailings (LZT). LZT is from the Skarn type lead-zinc mines. It is the tailings after secondary mineral processing. Figure 1 shows that the main mineral phases in LZT are hedenbergite ($\text{CaFe}(\text{Si}_2\text{O}_6)$), johannsenite (calcium manganese pyroxene, $\text{CaMn}(\text{SiO}_3)_2$), epidote ($\text{Ca}_2\text{FeAl}_2[\text{SiO}_4][\text{Si}_2\text{O}_7]\text{O}(\text{OH})$), diopside ($\text{CaMg}(\text{Si}_2\text{O}_6)$), calcite (CaCO_3) and quartz (SiO_2). Table 1 shows that the amount of SiO_2 in the LZT was approximately 47.66 %, leaching toxicity of heavy metals in LZT accordance with Chinese Standard GB/T 5085.3-2007 *Standard of Hazardous Waste Identification—leaching toxicity identification* and the radioactivity accordance with Chinese Standard 6566-2010 *Limit of radionuclides in building materials*. The remainder is 66.41% after LZT screened with a 0.08 mm square holes sieve. Ordinary Portland cement (OPC). The cement used is OPC with the strength grade of 42.5 which complies with the Chinese National Standard GB 175–1999. The chemical compositions and the physical properties of OPC are shown in Table 1 and Table 2, respectively.

Table 1: Chemical composition of raw materials (mass fraction, %)

Materials	SiO_2	Al_2O_3	Fe_2O_3	FeO	MgO	CaO	TiO_2	SO_3	MnO	Loss	Others
LZT	47.66	4.58	3.85	8.71	2.68	20.42	0.28	-	6.15	3.75	1.87
FGDW	3.16	1.35	0.47	0.09	7.49	33.38	-	45.70	-	8.28	0.06
FA	51.93	33.28	2.87	0.74	0.89	4.54	1.10	-	0.11	2.73	1.84
GBFS	35.54	11.48	0.39	0.54	6.39	41.45	0.50	-	1.09	0.87	1.72

Table 2: Physical properties of OPC

Fineness (residue on 80 μm sieve) /%	Normal consistency /%	Setting time /min		Stability	Flexural strength /MPa		Compressive strength /MPa	
		Initial setting	Final setting		3 d	28 d	3 d	28 d
22.13	26.20	110	210	qualified	5.4	8.7	20.9	52.8

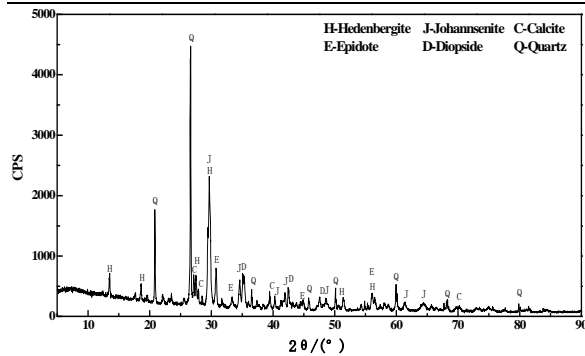


Figure 1: XRD spectra of LZT.

FA. It is class I FA. Its water demand is 92 % and its chemical composition is shown in Table 1. The main mineral phases include mullite and quartz, while there is a large amount of amorphous phase.

Ground blast furnace slag (GBFS). It is S95 GBFS, and it is complied with GB/T 18046-2000 *Ground granulated blast furnace slag used for cement and concrete*.

FGDW. Its chemical compositions are listed in Table 3. The primary mineral phase of FGDW is $\text{CaSO}_4 \cdot 2\text{H}_2\text{O}$. The specific surface area of the FGDW is $200 \text{ m}^2 \text{ kg}^{-1}$. And 0.08 mm sieve residual is less than 7.9%.

Aggregates. The coarse aggregates are crushed stones from magnetite-quartzite type iron mines. It has a particle size range is 3-19 mm with a mud content less than 0.3 % by mass, which is complied with GB/T 14685-2001 *Specification of pebble and crushed stone for building*. Fine aggregates are medium size sand for

construction, which is obtained after sieving the iron ore tailings of magnetite-quartzite type iron mines. It is compiled with GB/T 14684-2001 *Specifications of sand for building*.

Superplasticizer: It is PC high efficiency water reducer by Muhu Chemical Admixture LLC., Beijing, China.

2.2 Experimental methods

2.2.1 Preparation of LZT powder

LZT and FGDW were dried in oven (CS101–3E) at 105 °C for 24 h to achieve a moisture content less than 1 wt. %. Then they were grinded with the SM Φ 500 mm \times 500 mm 5 kg small ball grinder (WL-1) at the speed of 48 r \cdot min⁻¹. The grinding media consists of several steel balls and a steel forging. The grinding periods of LZT were chose to be 30 mins, 60 mins, 90 mins and 120 mins in order to obtain different specific surface area (SSA). According to the grinding periods, the obtained SSA of LZT were 350, 520, 600, and 680 m²kg⁻¹, respectively. FGDW was also grinded to a SSA of 380 m² kg⁻¹.

2.2.2 Preparation of mortars and concrete

Mortars: The cementitious materials for mortars are composed of OPC and LZT with different fineness as a mass ratio of 3:1. The water to cementitious material ratio is 0.4. And the content of superplasticizer is 0.3 % of cementitious materials by mass. The mixed fresh mortar was cast into the molds with the dimension of 40 mm \times 40 mm \times 160 mm, which were cured in moist room (RH>90 %, 20 \pm 1 °C) for 1 days. Then the demolded specimens were cured in lime water at 20 \pm 1 °C until specific ages (3 days, 7 days, and 28 days). The compressive and flexural strength of specimens was measured according to GB/T 50081-2002 *Standard for test method of mechanical properties on ordinary concrete*.

Concrete: The mixture proportion of C30 commercial concrete in Beijing is used as control as listed in Table 3. The ground LZT with the optimal fineness was blend in concrete replace cement, FA and GBFS, respectively, as a rate of 10 % by mass of the total cementitious materials. The mixture proportion are listed in Table 3. And the content of superplasticizer is 0.3 % of cementitious materials by mass. The flexural and compressive strength of concretes were measured at ages of 3 days, 7 days and 28 days.

Table 3: The mixture proportion of concrete with LZT

Group	OPC/ (kg m ⁻³)	FA/ (kg m ⁻³)	GBFS/ (kg m ⁻³)	LZT/(kg m ⁻³)	Sand/ (kg m ⁻³)	Stone/ (kg m ⁻³)	Slump/mm
1	240	80	80	0	870	960	20.0
2	200	80	80	40	870	960	20.5
3	240	40	80	40	870	960	19.0
4	240	80	40	40	870	960	20.0

2.2.3 Property characterizations

The particle size distribution of ground LZT was analyzed using laser particle size analyzer (MASTER SIZER 2000, the analysis range was 0.02~2000.00 μ m) with ethanol as the dispersant. The SSA of LZT was measured using dynamic specific surface area analyzer (SSA-3200). The compressive strength and flexural strength of the mortars were tested in reference to *Method of Testing Cements: Determination of Strength* (GB/T 17671-1999). The test of slump was measured using the Chinese standard GB/T2419-205. The strength was measured using hydraulic pressure testing machine (YES-300) with a maximum load of 300 KN and a loading rate of 2.0 \pm 0.5 kN/s. The XRD spectra were obtained using a D/Max-RC diffractometer (Japan) with Cu-K α radiation, voltage of 40 kV, current of 150 mA and 2 θ scanning ranging between 5 ° and 90 °. And the wavelength is 1.5406 nm. The autogenous shrinkage of concrete was measured with contactless concrete shrinkage strain gauge (CABR-NES, precision: \pm 1 μ m/m) according to the procedure in ref (Xiao et al., 2011). Chloride permeability and carbonation resistance was conducted based on GB/T 50082-2009 *Standard for test methods of long-term performance and durability of ordinary concrete*.

3. Results and discussion

3.1 Determination of grinding LZT fineness

3.1.1 The influence of grinding time on LZT fineness

Figure 2 shows the particle size distribution of ground LZT after different grinding time. For the grinding time of 30 mins, most of the particles are smaller than 60 μ m. As the grinding time increases, the particle size distribution gets narrower. After 60 mins grinding, most of the particles are smaller than 25 μ m. As the grinding time further increases, the particle size distribution becomes wider again. As of 120 mins grinding time, the particle size distribution is 0-40 μ m. The reason for the decreasing first and increasing later of particle size distribution is due to the agglomeration of fine LZT particles by electrostatic interaction. Figure 3 shows the

increasing specific surface area of the ground LZT as the grinding time increases. Considering the influence of particle agglomeration on the properties of concrete, strength tests on mortars with LZT are needed to determine the optimal grinding time.

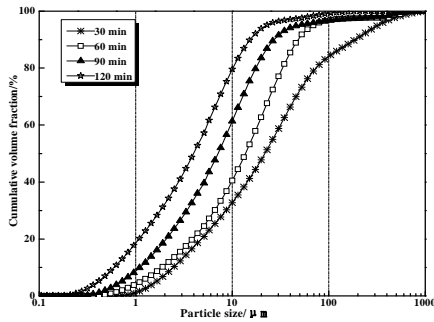


Figure 2: The particle size distribution of LZT.

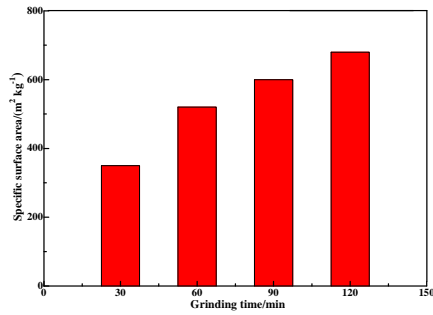


Figure 3: The SSA of LZT.

3.1.2 Strength of mortars with LZT

Figure 4 and Figure 5 show the flexural strength and compressive strength of the mortars with LZT. As the grinding time increases, both flexural and compressive strength increases first and decreases later. As of the concrete with the LZT of 60 mins grinding, the compressive strength at the age of 28 days is higher than 40 MPa. However, the compressive strength of the concrete with LZT of 120 mins is 32.5 MPa at the age of 28 days. This is due to the agglomeration of fine particles by the electrostatic interaction. The electrostatic interaction will also influence the particles of other materials, such as cement, FA and GBFS, which may have a negative impact on the mechanical properties of the concrete. Thus, the optimal SSA of LZT was determined to be 520 m² kg⁻¹.

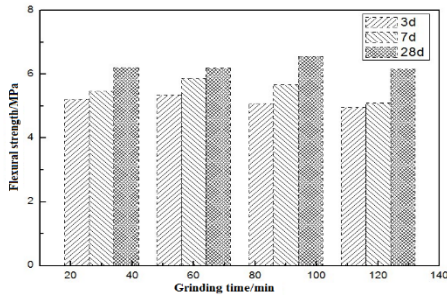


Figure 4: The flexural strength of mortars.

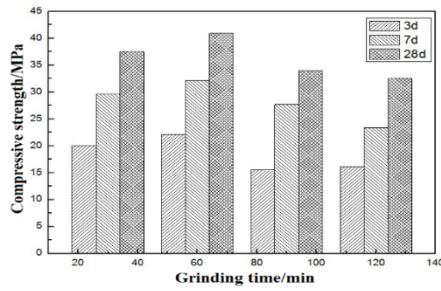


Figure 5: The compressive strength of mortars.

3.2 Strength of concrete with LZT

Figure 6 shows the compressive strength of concrete with LZT.

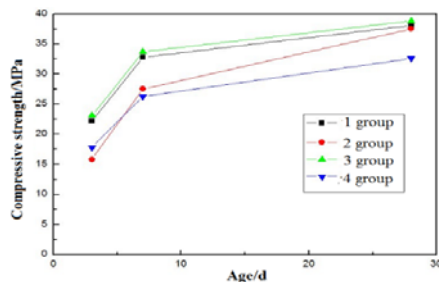


Figure 6: The compressive strength of concrete with LZT replacing cement, FA and GBFS, respectively.

Group 3 (replacing FA by LZT) shows the highest compressive strength with a value of 37.8 MPa, which is slightly higher than the control (36.8 MPa). As a mineral admixture, FA exhibits physical effect, micro-filler effect and pozzolanic reactivity. Since the ground LZT is finer than FA, there shows a better micro-filler effect and pozzolanic reactivity. This better helps densify the microstructure of the concrete. Overall, three concretes

with LZT all have a strength higher than 30 MPa at the age of 28 days, which is compiled with the requirement of C30.

3.3 Durability of concrete with LZT

3.3.1 Chloride permeability

Table 4 lists the result of chloride permeability. The low coulombs passed through the concrete with LZT indicates their low chloride permeability. In the particle packing structure of the unhydrated cementitious materials, there are a lot of smaller voids less than 5 μm . Considering the size of more than 60 % LZT particle are smaller than 5 μm , it can effectively fill the voids, which decreases the capillary porosity, which densifies the microstructure of the concrete. Meanwhile, $\text{Ca}(\text{OH})_2$ can react with the mineral admixtures to produce the low alkalinity, stable and hardly soluble C-S-H gels. Thus, the C-S-H gels is able to improve the pore structure of the interfacial zone due to the pozzolanic reaction.

Table 4: Chloride permeability of concrete with LZT

Coulombs	High	Medium	Low	Very low	Negligible
Chloride permeability	>4000	2000~4000	1000~2000	100~1000	<100
Test results	-	-	-	908	-

3.3.2 Carbonation resistance

Carbonation of concrete is a process of reactions between the mineral phases (mainly $\text{Ca}(\text{OH})_2$, C-S-H gels, C_3S and C_2S) and CO_2 from the external environment. The reactions are shown below:



Table 5: Carbonation depth of concrete with LZT

Time/Day	3 d	7 d	14 d	28 d
Carbonation depth/mm	1.0	3.3	5.7	7.0

Table 5 lists the carbonation depth of the concrete with LZT, which indicates that it has a good carbonation resistance. It is complicated to address the influence of mineral admixtures on carbonation. Firstly, the addition of mineral admixtures lowers the alkalinity of the system, which is bad to resist carbonation. On the other hand, the pozzolanic reaction decreases the porosity, which increase the carbonation resistance. Moreover, the concrete with multiple mineral admixtures shows better carbonation resistance compared to the concrete with a single mineral admixture. This is due to that the varying particle size distribution of the multiple mineral admixtures make a denser microstructure. The LZT used here has a fine particle size distribution, which better helps densify the microstructure and improve its pozzolanic reactivity. Thus, the addition of LZT helps increase the carbonation resistance of concrete.

3.3.3 Autogenous shrinkage

Autogenous shrinkage is due to the capillary pressure resulting from emptying capillary pores during hydration..

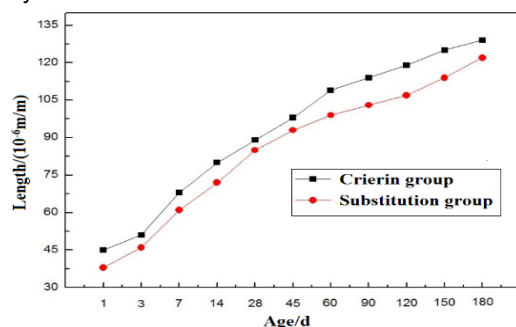


Figure 7: The autogenous shrinkage of the concrete with LZT (10⁻⁶m/m).

Figure 7 shows the autogenous shrinkage of the concrete with LZT. There is smaller autogenous shrinkage after 1 days hydration compared to that of the control. This maybe result from the micro-filler effect of LZT, the change in hydration heat, the change in hydrate composition. More work needs to be done to illustrate the mechanism of the change in autogenous shrinkage

4. Conclusions

- (1) As the grinding time increases, the agglomeration of the fine particles occurs, which is bad to the mechanical properties of the mortars with LZT.
- (2) The requirement of C30 is met in all the concrete with LZT partially replacing cement, FA, GBFS, respectively.
- (3) Due to the fine particle size distribution of LZT (more than 60 % particles are smaller than 5 μm), it shows a good micro-filler effect, which densifies the microstructure of the concrete, improves the pore network of the interfacial zone. Thus, better durability is achieved in concrete with LZT.

Acknowledgments

The authors gratefully acknowledge financial support from China Postdoctoral Science Foundation (2016M602082), supported by Science and Technology Research Project of Higher Education Universities in Hebei Province (ZD2016014, QN2016115), supported by Construction Science and Technology Foundation of Hebei Province (2012-136), supported by Handan Science and Technology Research and Development Plan Program (1621211040-3), supported by Jiangxi Postdoctoral Daily Fund Project (2016RC30).

Reference

- Anastasiou E., Filiksa K.G., Stefanidou M., 2014, Utilization of fine recycled aggregates in concrete with fly ash and steel slag, *Construction and Building Materials*, 50, 154-161, DOI:10.1016/j.conbuildmat.2013.09.037.
- Bobylev N., 2009, Mainstreaming sustainable development into a city's Master plan: A case of Urban Underground Space use, *Land Use Policy*, 26(4), 1128-1137, DOI: 10.1016/j.landusepol.2009.02.003.
- Cui X.W., Wang C.L., Ni W., Di Y.Q., Cui H.L., Chen L., 2017, Study on the reaction mechanism of autoclaved aerated concrete based on iron ore tailings, *Romanian Journal of Materials*, 47(3), 46-53 (in Romania).
- Liu H.X., Wang C.L., Chen L., Liu S.C., Yang J., 2016, Preparation and properties of autoclaved sand-bricks using iron ore tailings and waste rock. *Journal of Mines, Metals & Fuels*, 63(12), 681-686.
- Nematollahi B., Sanjayan J., 2014, Effect of different superplasticizers and activator combinations on workability and strength of fly ash based geopolymer, *Materials and Design*, 57(5), 667-672, DOI: 10.1016/j.matdes.2014.01.064.
- Shetty K.K., Nayak G., Vijayan V., 2014, Effect of red mud and iron ore tailings on the strength of self-compacting concrete, *European Scientific Journal*, 10, 168-176.
- Ugama T.I., Ejeh S P., Amartey D.Y., 2014, Effect of iron ore tailing on the properties of concrete, *Civil and Environmental Research*, 6(10), 7-12.
- Upadhyaya S., Goulias D., Obla K., 2015, Maturity-based field strength predictions of sustainable concrete using high-volume fly ash as supplementary cementitious material, *Journal of Materials in Civil Engineering*, 27(5), 69-75, DOI: 10.1061/(ASCE)MT.1943-5533.0001123.
- Wang C.L., Ni W., Zhang S.Q., Wang S., Gai G.S., Wang W.K., 2016, Preparation and properties of autoclaved aerated concrete using coal gangue and iron ore tailings, *Construction and Building Materials*, 104(1), 109-115, DOI: 10.1016/j.conbuildmat.2015.12.041.
- Wang C.L., Zheng Y.C., Liu S.C., Yang J., 2015, Microstructure and mechanical properties of glass-ceramics prepared with coal gangue and iron ore tailings, *Rare Metal Materials and Engineering*, 44, 234-238 (in China) .
- Xiao J., Chen L., Xing H., 2011, Influence of fly ash and slag powder on autogenous shrinkage of cement mortars, *Journal of Building Materials*, 14(5), 604-609 (in China), DOI: 10.3969/j.issn.1007-9629.2011.
- Zhang J.W., Wang C.L., Liu H.X., Zhong W., Chen L., Qian W., Liu Z.Y., 2016, Study of preparation for autoclaved aerated concrete with low-silica iron ore tailings. *Revista de la Facultad de Ingenieria*, 31(12), 36-48.
- Zhao H., Sun W., Wu X.M., Gao B., 2015, The properties of the self-compacting concrete with fly ash and ground granulated blast furnace slag mineral admixtures, *Journal of Cleaner Production*, 95, 66-74, DOI: 10.1016/j.jclepro.2015.02.050.